Electronic Supplementary Material (ESI) for Nanoscale Horizons.

SUPPORTING INFORMATION

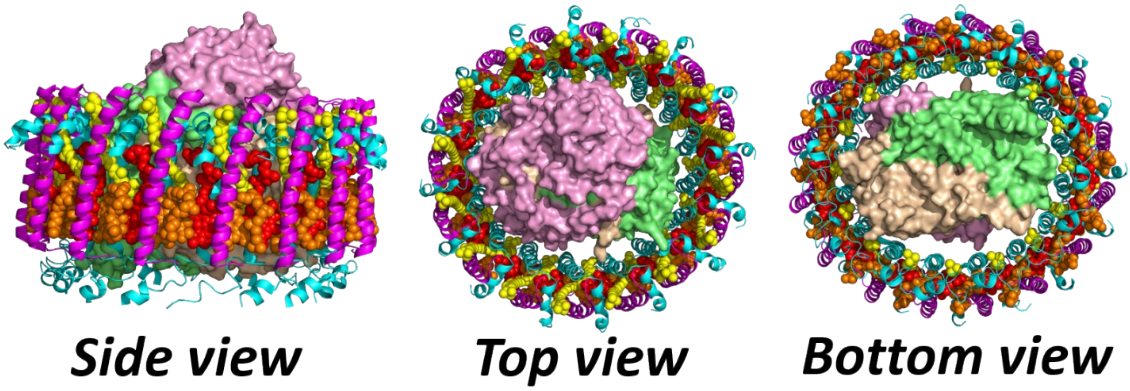

Figure S1. Architecture of the RC-LH1 complex. *Three views of the RC-LH1 complex in which a hollow cylinder of LH1 pigment protein surrounds a central RC domain. The RC is shown as a solid object with the three component polypeptides colored pink, green and beige. These proteins form a scaffold for the electron transfer cofactors that carry out photochemical charge separation. The LH1 domain comprises concentric cylinders of 16 alpha and beta polypeptides (cyan and magenta ribbons, respectively) that hold in place rings of light harvesting carotenoid molecules (yellow spheres) and bacteriochlorophyll molecules (spheres, alternating red and orange).*

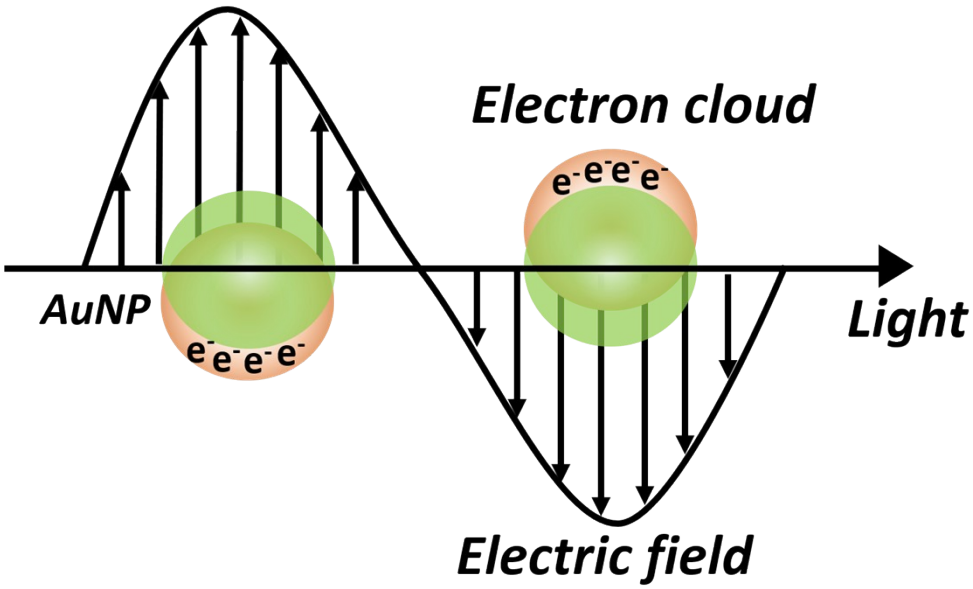

Figure S2. Schematic demonstrating localised surface plasmon resonance in which free electrons in the metal NP oscillate due to strong coupling with incident light.

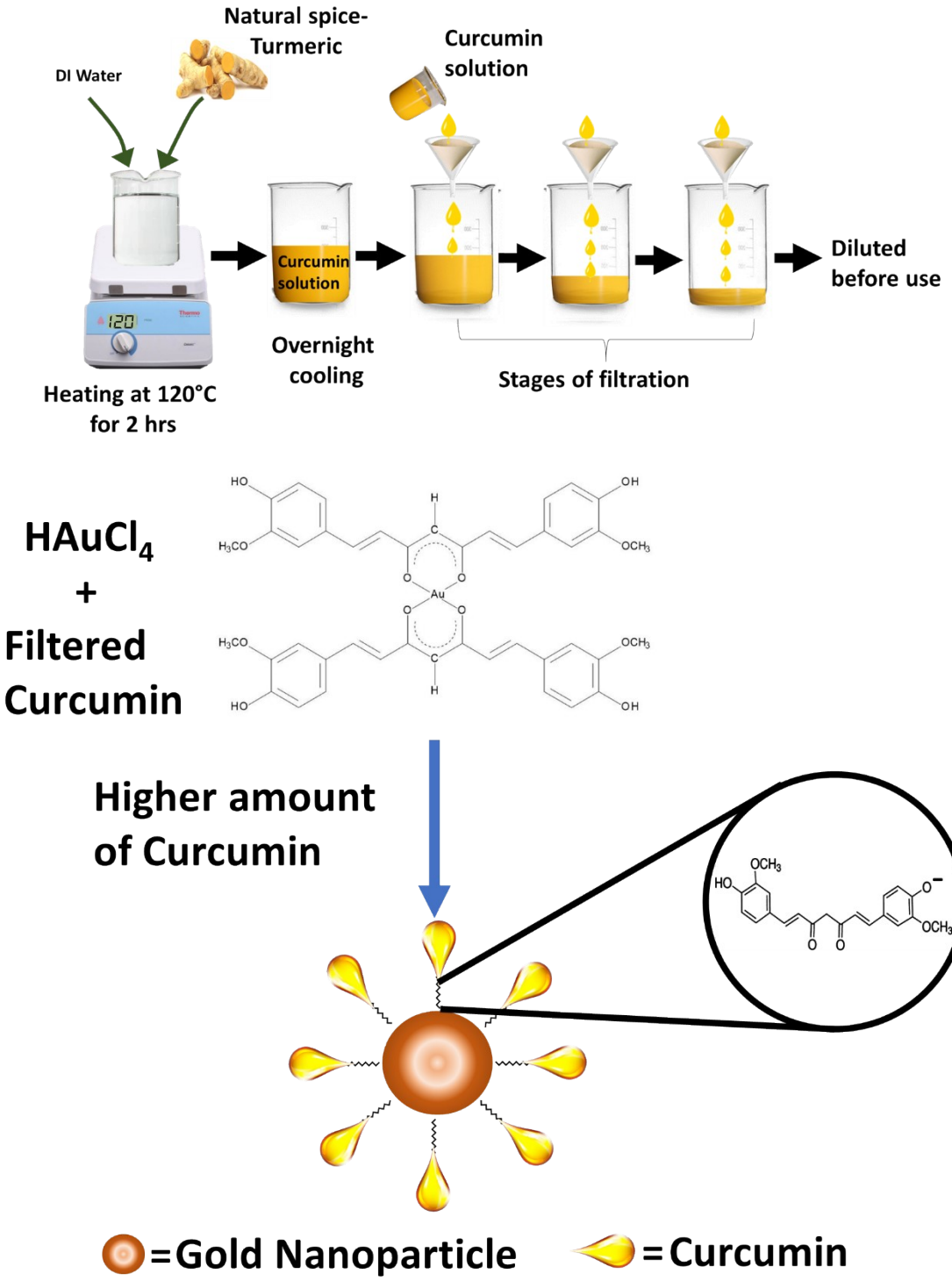

Figure S3. Schematic showing the formation of curcumin stabilized gold NPs.

-

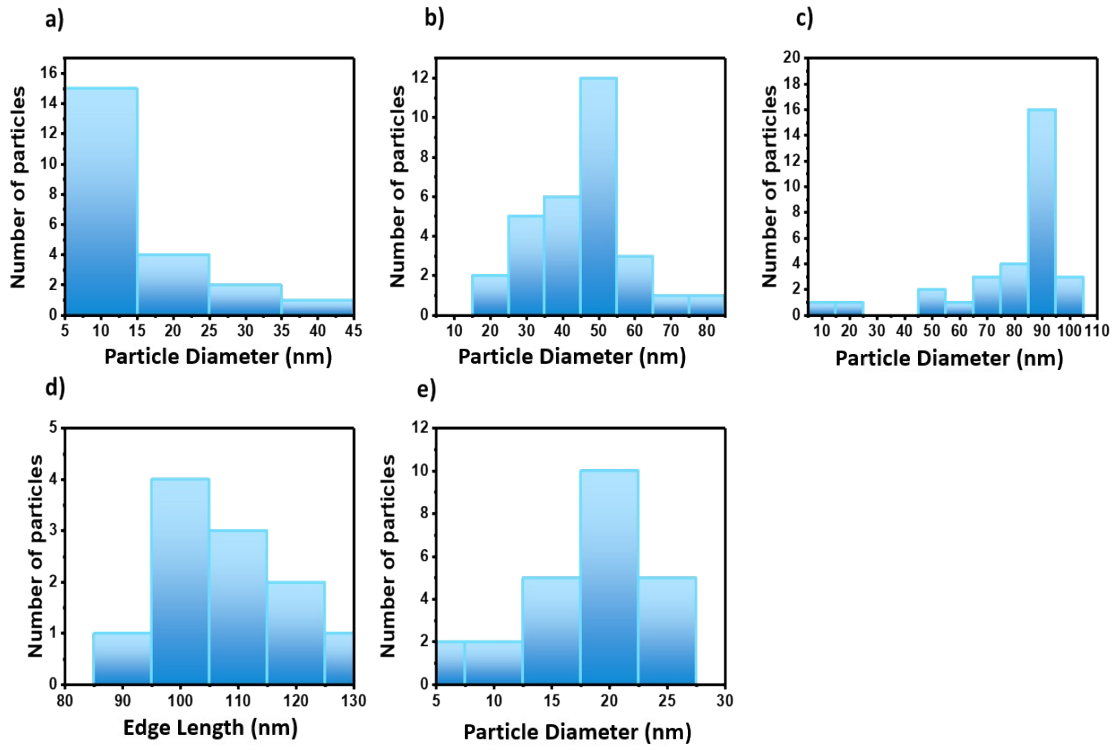

Figure S4*. Distributions of gold NP size. (a)** *Spherical NPs obtained after overnight stirring (NPs-10).* ***(b) *Spherical NPs obtained after 90 mins stirring (NPs-50).* ***(c)*** *Spherical NPs obtained after 30 mins stirring (NPs-90).* ***(d)*** *Triangular NPs obtained after overnight stirring at pH 4 (NPs-T).* ***(e)*** *Star-shaped NPs obtained in the presence of hydroxylamine (NPs-S). The diameter of the NPs-T particles was determined by measuring the length of one of the edges, while for the NPs-S particles the diameter was the average of the distance between any two peaks/corners from the TEM image.*

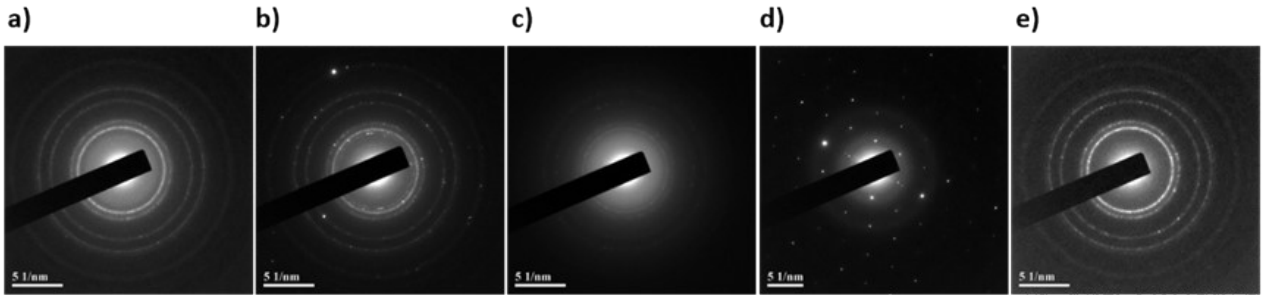

***Figure S5**. **Nanoparticle characterization. (a-e)** SAED images of NPs-10 (a), NPs-50 (b), NPs-90 (c), NPs-T (d) and NPs-S (e) particles.*

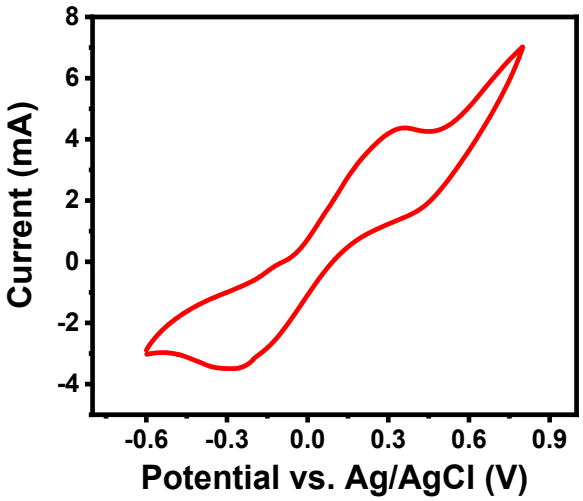

***Figure S6**. **Voltammetry of electrolyte.** Cyclic voltammogram of 100 mM TMPD in 0.01 mM Tris- HCl (pH 7.5).*

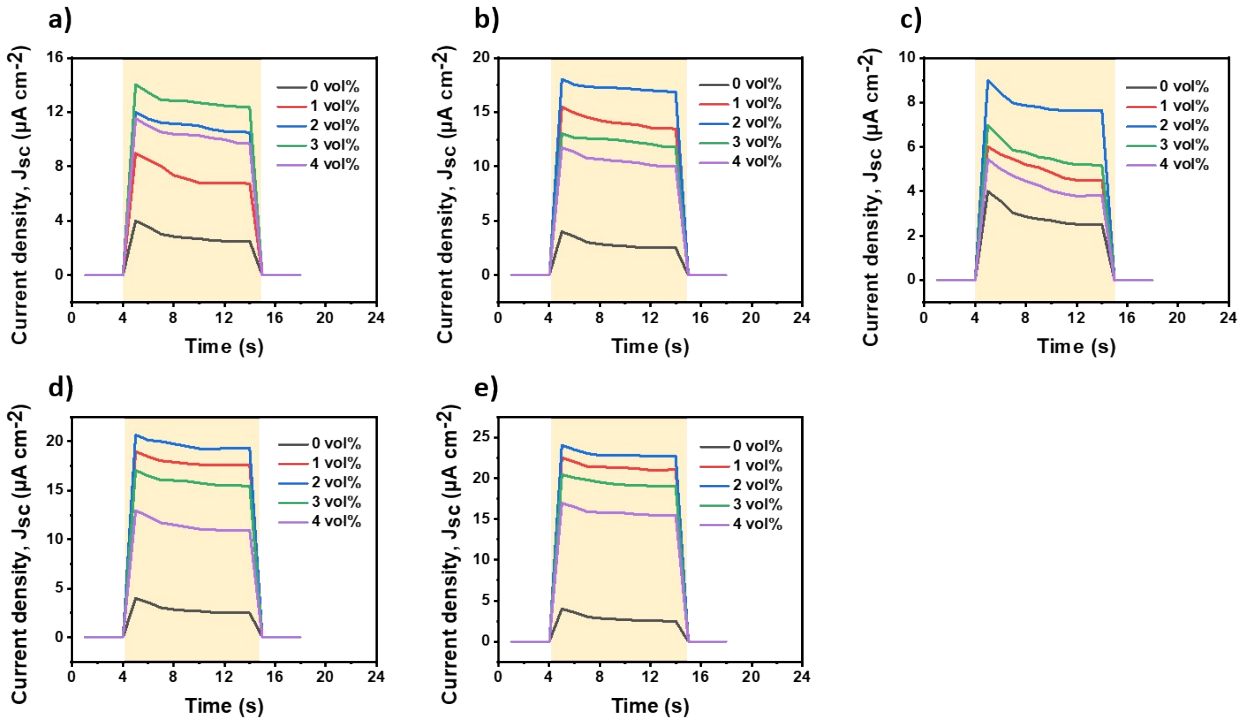

Figure S7. J_{sc} from RC-LH1 cells without and with 0 to 4 vol% gold NPs. *Effect of* ***(a)*** *NPs-10,* ***(b)*** *NPs-50,* ***(c)*** *NPs-90,* ***(d)*** *NPs-T,* ***(e)*** *NPs-S NPs. Shaded areas indicate periods of AM 1.5 illumination at 100 mW/cm^2. Data shown are the average of five measurements under identical test conditions.*

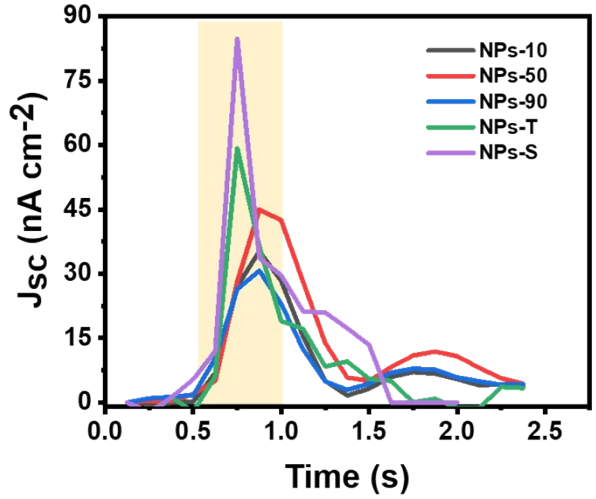

Figure S8. No-protein controls for cells with a tungsten back electrode. *J_{sc} from cells with different types of NPs fabricated using bare tungsten electrode in the absence of RC-LH1. Shaded area indicates a period of AM 1.5 illumination at 100 mW/cm^2.*

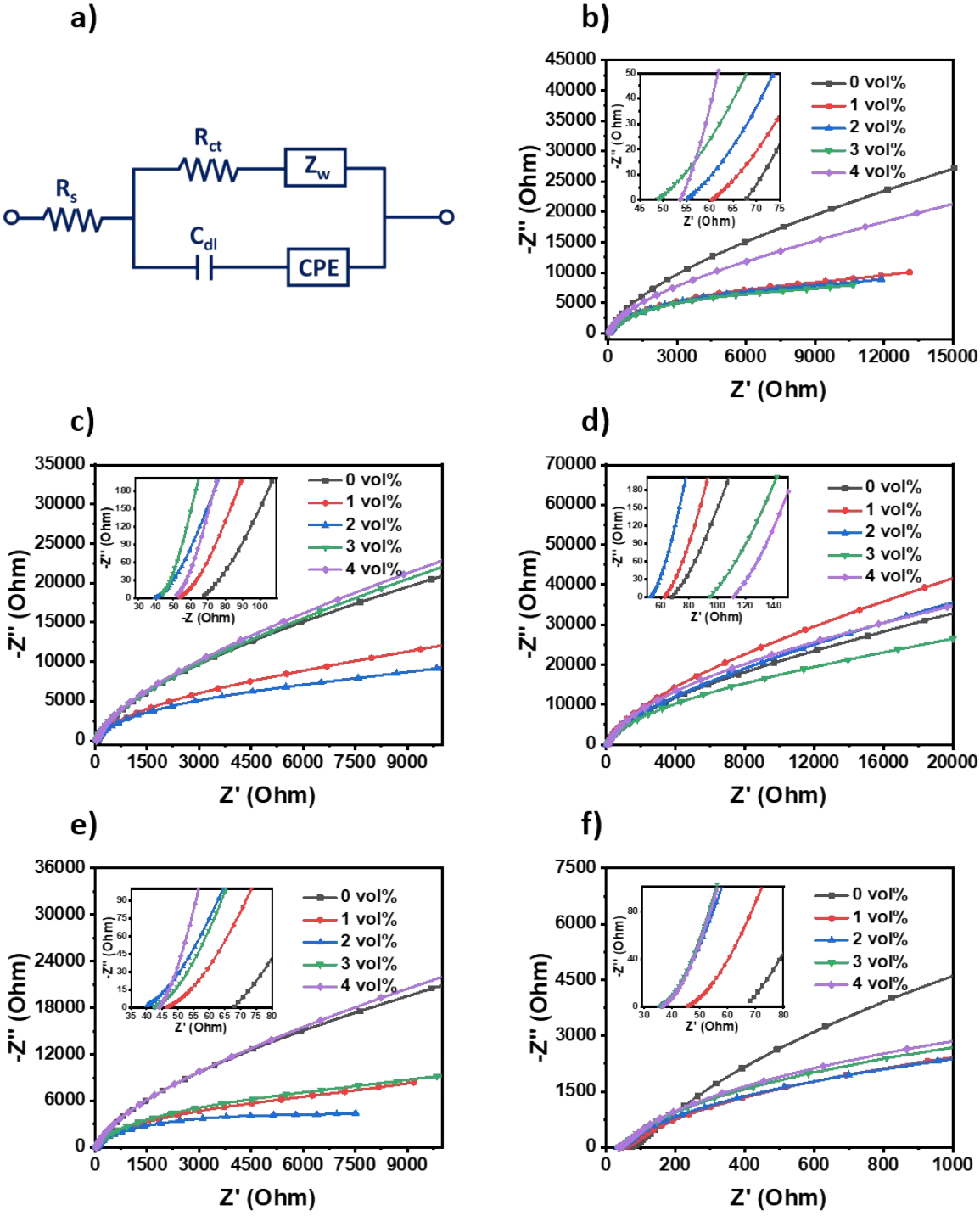

Figure S9. EIS of RC-LH1 cells with gold NPs. (a) *Randles equivalent circuit model used to fit EIS spectra of the cells. Parameters are the sheet resistance of device (R_s), charge transfer resistance at the electrode-electrolyte surface (R_{ct}), Warburg constant resulting from charge diffusion to the electrode (Z_w) and electrical double layer capacitance (C_{dl}). A constant phase element (CPE) acts as a non-ideal capacitor, which is used to account for inhomogeneities on the tungsten electrode surface.* ***(b-f)*** *Complex impedance plots for RC-LH1 cells with 0 to 4 vol% gold NPs. Cells were doped with NPs-10 (b), NPs-50 (c), NPs-90 (d), NPs-T (e) and NPs-S (f) gold NPs.*

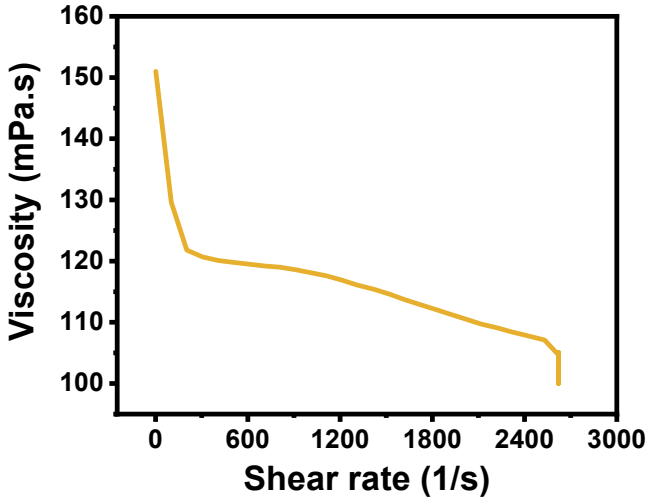

Figure S10. Viscosity versus shear rate profile of the formulated silver ink analysed at room temperature.

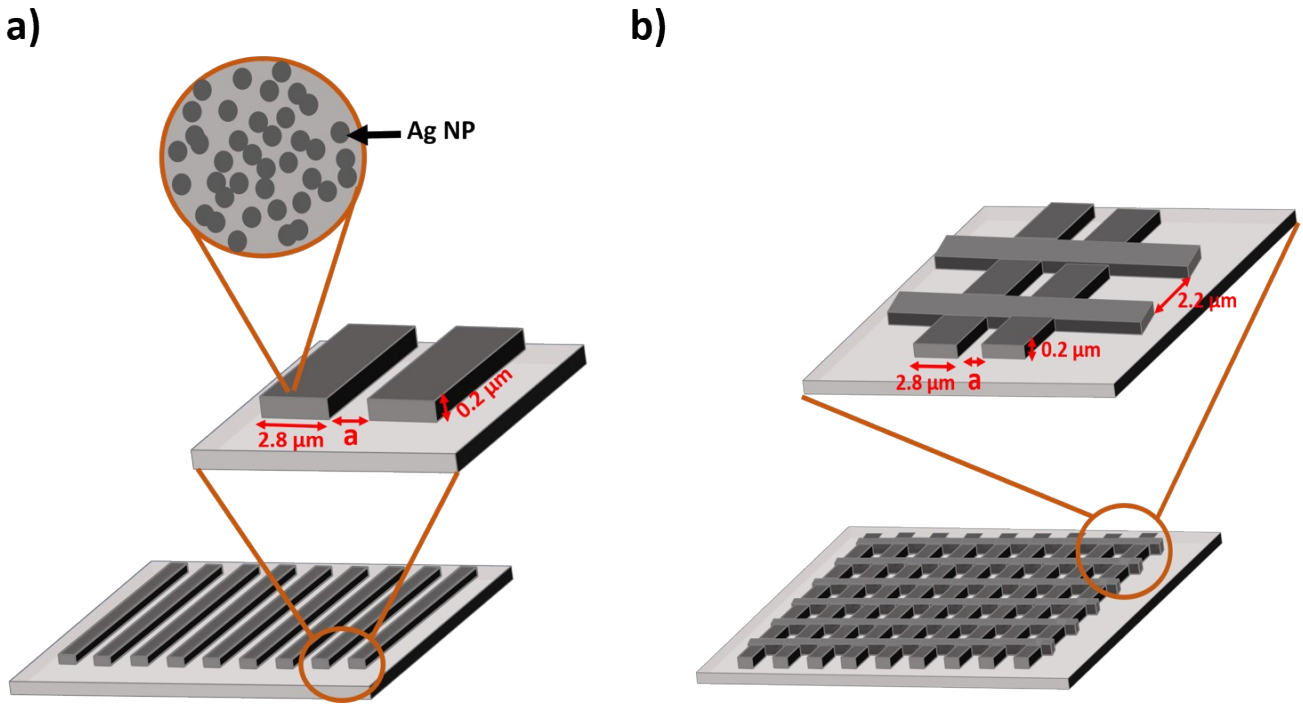

Figure S11. Schematics of the patterned electrodes.

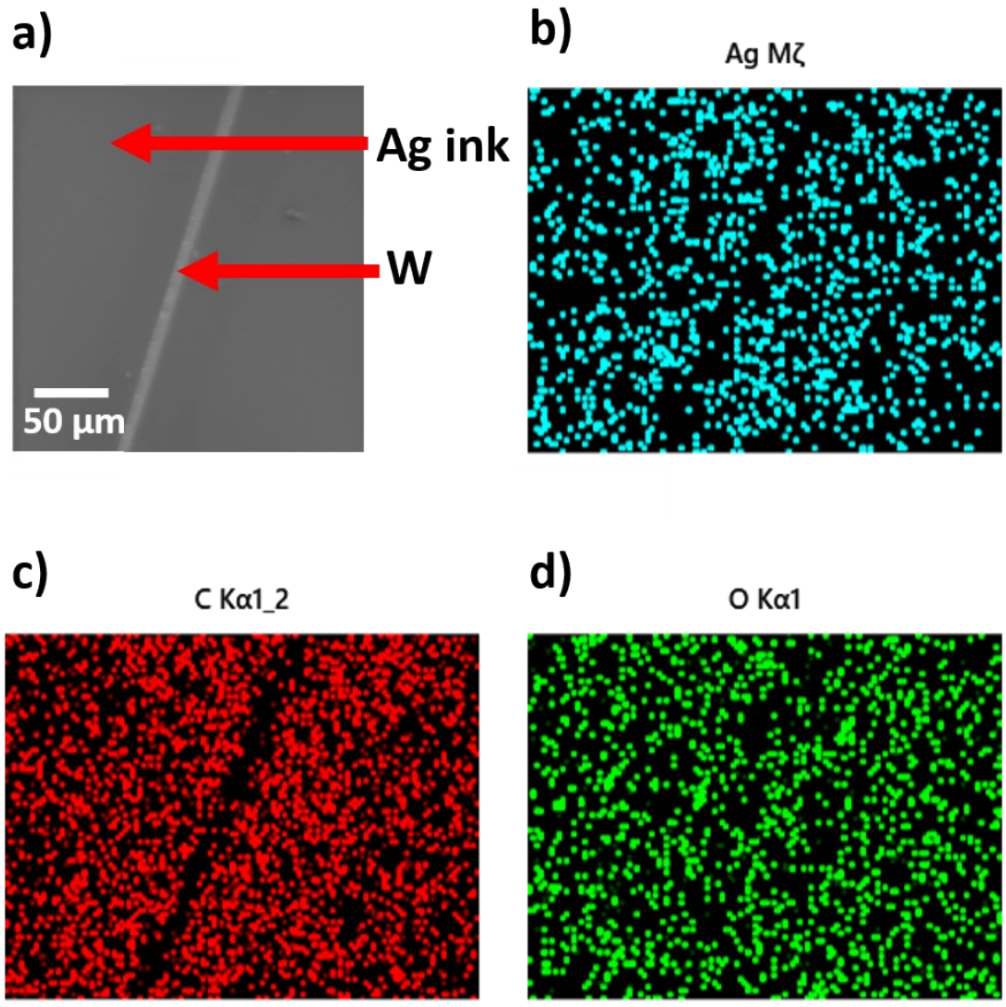

Figure S12. EDS mapping of the printed silver patterns. (a) *SEM image,* ***(b-d)*** *the corresponding elemental mapping of Ag, C, O, respectively.*

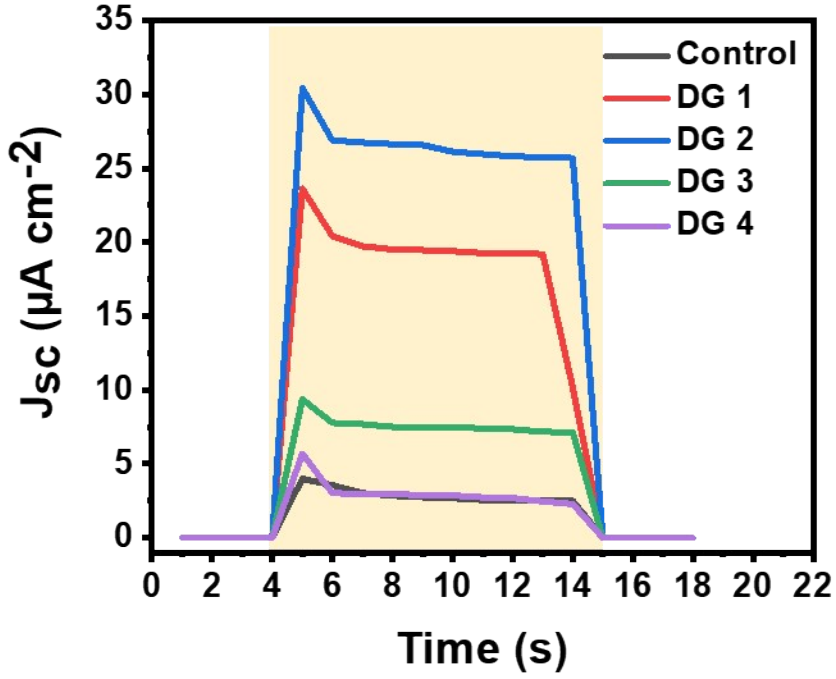

Figure S13. Effect of a naopatterned back electrode. *J_{sc} of RC-LH1 cells with different patterned back electrodes, measured under AM 1.5 illumination at 100 mW/cm^2 (shaded period). Data shown are the average of five measurements under identical test conditions.*

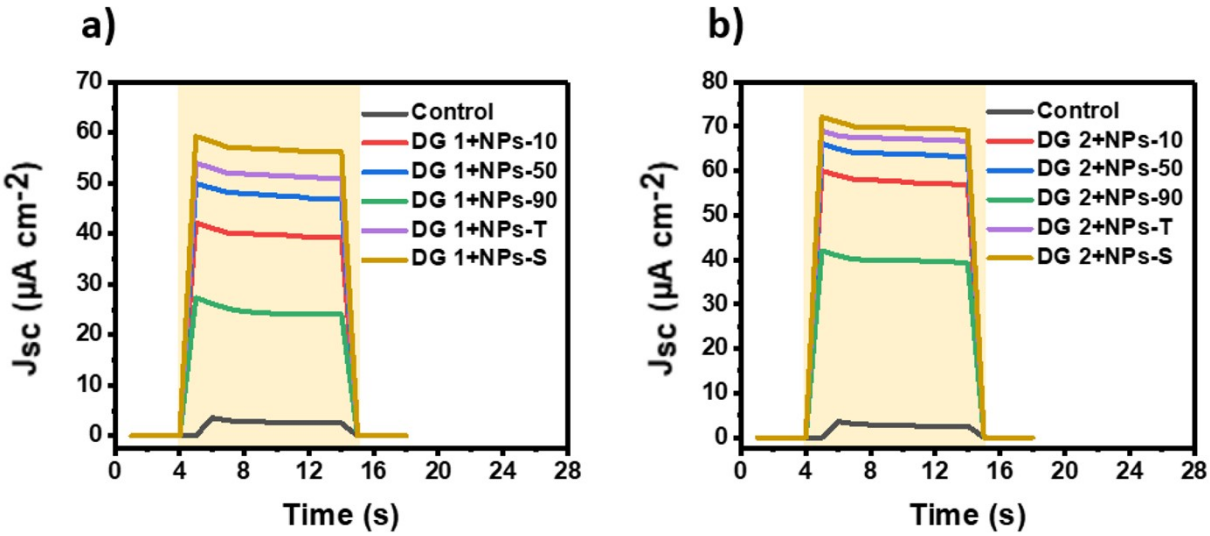

Figure S14. Performance of Protein Electricity Generator with a nanopatterned back electrode*. **(a)** J_{sc} of RC-LH1/gold NP cells with a DG-1 patterned back electrode, measured under AM 1.5 illumination at 100 mW/cm^2 (shaded period). **(b)** J_{sc} of RC-LH1/gold NP cells with a DG-2 patterned back electrode, measured as for (a). Data shown are the average of five measurements under identical test conditions.*

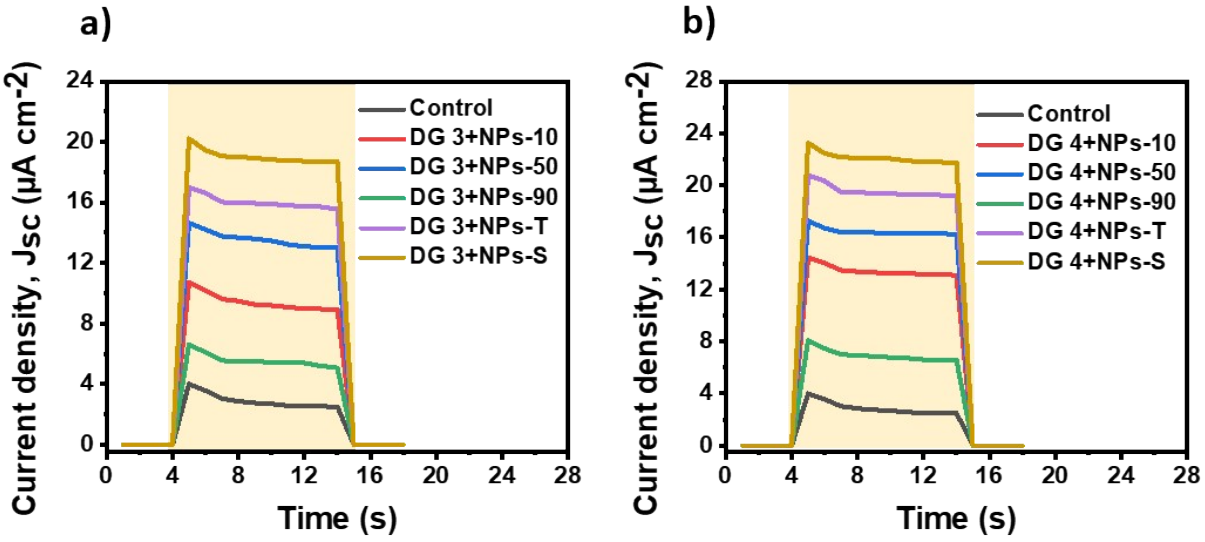

Figure S15. Performance of Plasmonic Protein Electricity Generator with a nanopatterned back electrode. ***(a)*** *J_{sc} of RC-LH1/gold NP cells with a DG-3 patterned back electrode, measured under AM 1.5 illumination at 100 mW/cm^2 (shaded area).* ***(b)*** *J_{sc} of RC-LH1/gold NP cells with a DG-4 patterned back electrode, measured as in (a). Data shown are the average of five measurements under identical test conditions.*

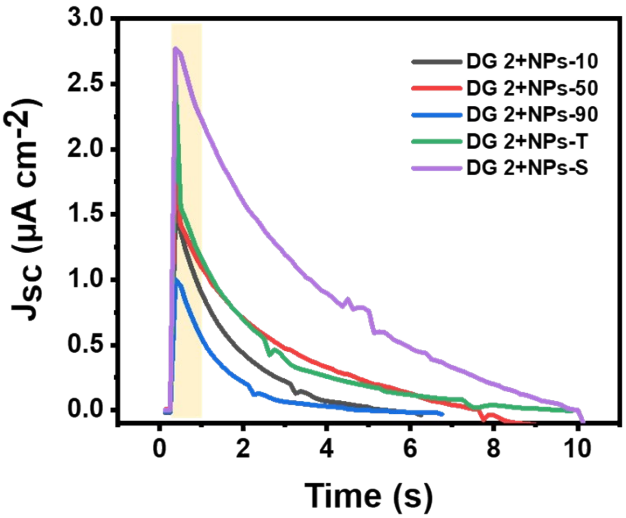

Figure S16. No-protein controls for cells with a nanopatterned back electrode. *J_{sc} from cells with different types of NPs fabricated using DG-2 patterned tungsten electrode in the absence of RC-LH1. Shaded area indicates a period of AM 1.5 illumination at 100 mW/cm^2.*

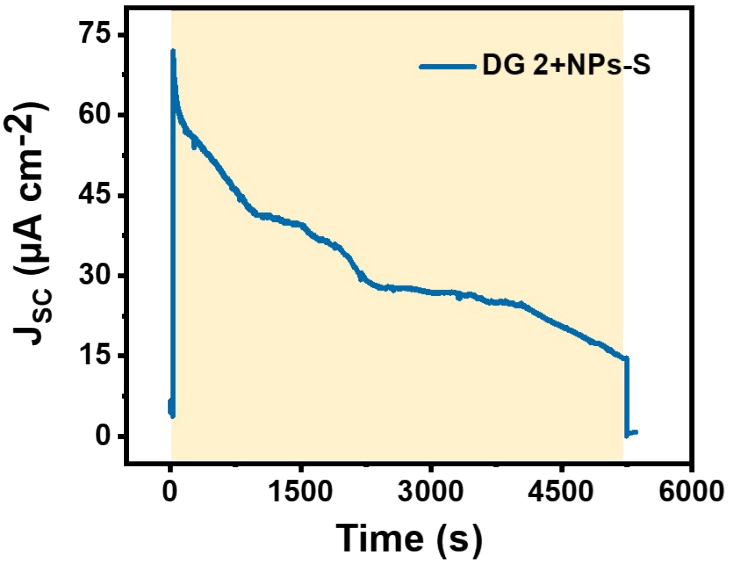

Figure S17. Stability of output. *J_{sc} measured over a long light soaking time for a cell fabricated using star-shaped AuNPs and DG-2 back electrode. Shaded area indicates a period of AM 1.5 illumination at 100 mW/cm^2.*

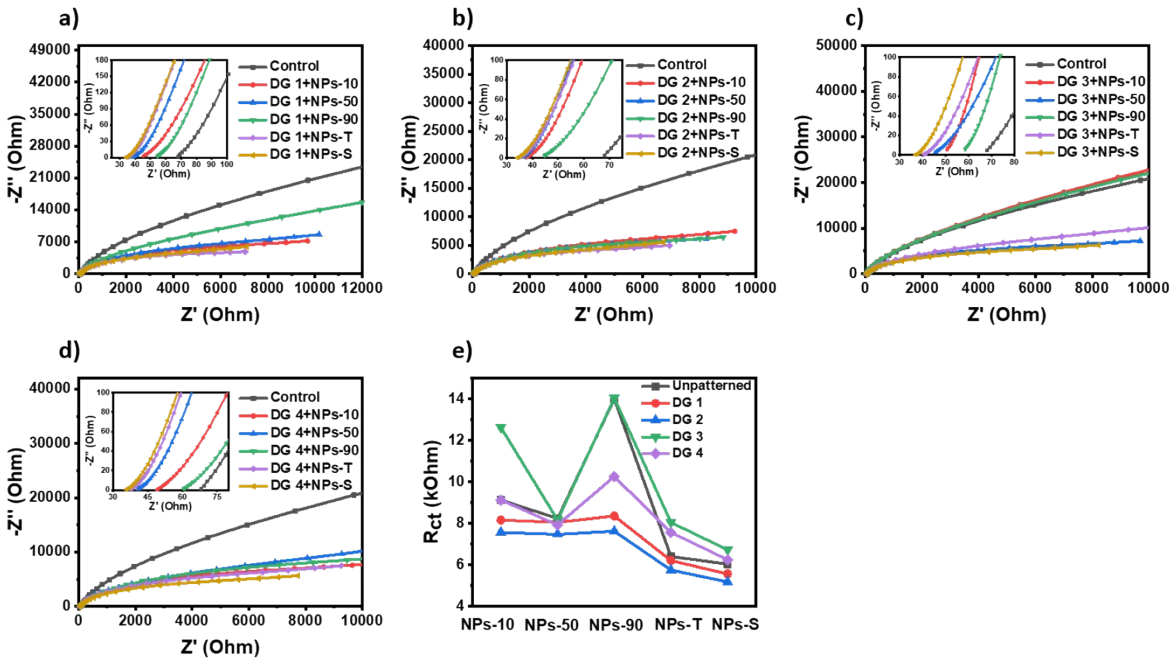

Figure S18. EIS of Protein Electricity Generator with gold NPs and a nanopatterned back electrode. (a-d) *Complex impedance plots for RC-LH1 cells with a patterned back electrode, without and with an optimized concentration of gold NPs. Cells were fabricated with a DG-1 electrode (a), DG-2 electrode (b), DG-3 electrode (c) and DG-4 electrode (d).* ***(e)*** *Charge transfer resistances of photovoltaic cells fabricated with four different types of patterned back electrode and five different gold NPs.*

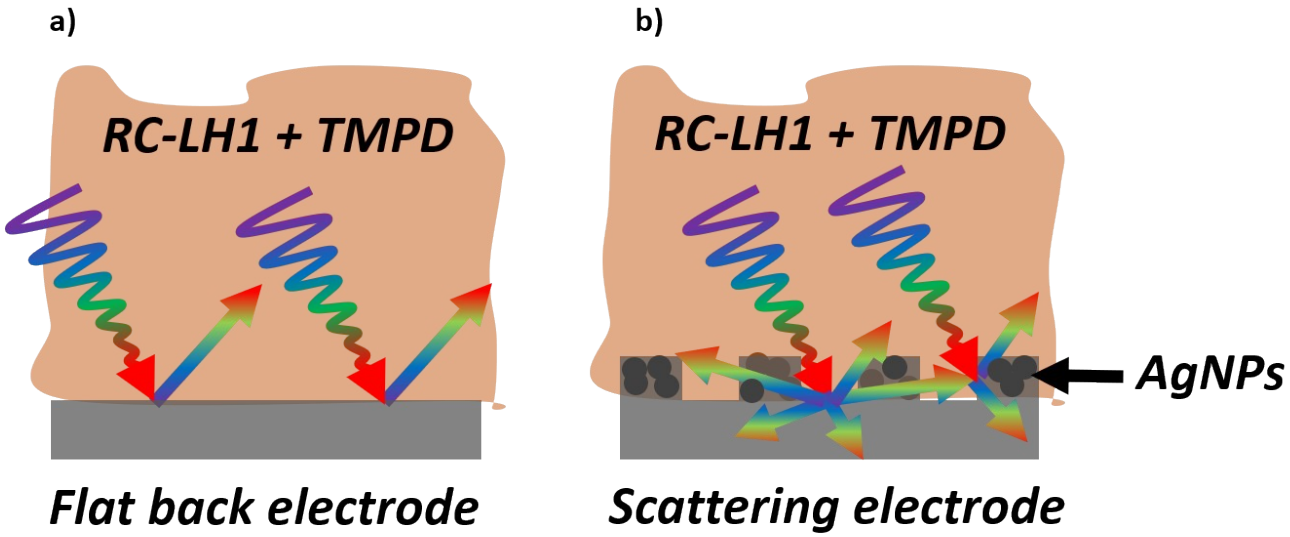

Figure S19. Light behaviour in Protein Electricity Generator. ***(a)*** *In control RC-LH1 cells formed from a planar tungsten electrode some of the incoming light is reflected back into the protein-electrolyte matrix.* ***(b)*** *In cells with a nanopatterned rear electrode more complex scattering from bottom electrode surface structures and grooves occurs, increasing the optical path of the incoming light and thereby enhancing light absorption.*

***Table S1**. Conductivity, electrophoretic mobility and zeta potentials of the NPs.*

Device	Conductivity (mS/cm)	Electrophoretic mobility (μm*cm/Vs)	Mean zeta potential (mV)
NPs-10	0.14	-1.1	-14.05
NPs-50	0.14	-1.4	-17.84
NPs-90	0.14	-1.4	-17.58
NPs-T	0.13	-1.3	-16.61
NPs-S	16.21	-2.1	-27.31

***Table S2**. Parameters for RC-LH1 cells fabricated with DG-1 patterned electrodes.*

Device	J_{sc} (μA/cm^2)	V_{oc} (V)	η (%)*10^{-3}	R_S (Ω)	R_{ct} (Ω)
Control	23.62	0.28±0.01	6.6	46	16140
DG-1+NPs-10	41	0.3±0.01	12.26	43.07	8161
DG-1+NPs-50	50	0.3±0.01	15	37.85	8054
DG-1+NPs-90	27	0.3±0.01	8.05	52.44	8358
DG-1+NPs-T	55	0.3±0.01	16.3	34.75	6307
DG-1+NPs-S	60	0.3±0.01	17.94	33.37	5561

***Table S3**. Parameters for RC-LH1 cells fabricated with DG-2 patterned electrodes.*

Device	J_{sc} (μA/cm^2)	V_{oc} (V)	η (%)*10^{-3}	R_S (Ω)	R_{ct} (Ω)
Control	30.4	0.28±0.01	8.5	39.3	12160
DG-2+NPs-10	60	0.3±0.01	18.12	36.99	7565
DG-2+NPs-50	67	0.3±0.01	20	35.28	7463
DG-2+NPs-90	42	0.3±0.01	12.6	42.5	7623
DG-2+NPs-T	69	0.3±0.01	20.7	34.29	5750
DG-2+NPs-S	73	0.3±0.01	21.83	33.46	5174

***Table S4**. Parameters for RC-LH1 cells fabricated with DG-3 patterned electrodes.*

Device	J_{sc} (μA/cm^2)	V_{oc} (V)	η (%)*10^{-3}	R_S (Ω)	R_{ct} (Ω)
Control	9.27	0.28±0.01	2.62	248.5	46350
DG-3+NPs-10	10.5	0.3±0.01	3.15	48.03	12630
DG-3+NPs-50	14.5	0.3±0.01	4.35	43.07	8161
DG-3+NPs-90	6.5	0.29±0.01	1.90	55.2	14045
DG-3+NPs-T	17	0.29±0.01	4.96	39.91	8045
DG-3+NPs-S	20	0.3±0.01	6.00	36.31	6722

***Table S5**. Parameters for RC-LH1 cells fabricated with DG-4 patterned electrodes.*

Device	J_{sc} (μA/cm^2)	V_{oc} (V)	η (%)*10^{-3}	R_S (Ω)	R_{ct} (Ω)
Control	5.68	0.28±0.01	1.59	70.44	21910
DG-4+NPs-10	14.45	0.29±0.01	4.22	46.18	9126
DG-4+NPs-50	17.5	0.29±0.01	5.1	39.91	7925
DG-4+NPs-90	8	0.29±0.01	2.34	53.5	10260
DG-4+NPs-T	20.75	0.3±0.01	6.23	36.99	7565
DG-4+NPs-S	23	0.3±0.01	6.9	35.02	6247